

## FAST TIME-OF-FLIGHT SYSTEM FOR MUON COOLING EXPERIMENTS\*

R. J. Abrams<sup>#</sup>, C. M. Ankenbrandt, G. Flanagan, S. Kahn, M. Notani, T. J. Roberts  
Muons, Inc., Batavia, IL, U.S.A.

H. J. Frisch, University of Chicago, Chicago, IL, U.S.A.

### Abstract

A new generation of large-area, low cost time-of-flight detectors with time resolutions  $\leq 10$  ps and space resolutions  $\leq 1$  mm is being developed for use in nuclear and particle physics experiments, as well as for medical and industrial applications. Such detectors are being considered for use in muon cooling channel tests. Designs and fabrication of prototype planes and associated readout electronics are described. Results of simulations of time and space resolutions are presented.

### INTRODUCTION

The development of fast, large area, low cost time of flight detectors with excellent spatial resolution is developing rapidly. Prototype detectors with areas of  $\sim 1$  m<sup>2</sup> are expected to become available for testing and early applications in the next year or two. One of the applications that is attractive for early testing is the use in muon cooling experiments. The University of Chicago and Muons, Inc. are members of a multi-institutional collaboration LAPPD [1] that is developing fast TOF detectors based on micro-channel plates and fast electronics to realize the objectives of time resolutions  $\leq 10$  ps and space resolutions  $\leq 1$  mm for several applications.

### CHARACTERISTICS OF FAST TOF SYSTEM

The prototype detectors are shown in Figure 1. Each super-module is composed of six tiles, each 20 cm by 20 cm in size, mounted in a tray, 40 cm by 60 cm in size. The tiles have an entrance window, which also serves as a Cherenkov radiator, a photo-cathode to convert the Cherenkov light into electrons, a pair of micro-channel plates (MCP) with voltages applied to amplify the signal, and an exit window, which has electrodes to form a strip-line to carry the signal to the readout electronics. There are 80 electronics channels at each end of the strip-lines.

The layout of the clock and readout system for a super-module is shown in Figures 2 and 3. The overall system, which consists of four super-modules, is controlled by the same digital card. Simulations have shown that the overall system, including the clock and readout system can meet the requirements of time resolutions  $\leq 10$  ps and space resolutions  $\leq 1$  mm.



Figure 1: Prototypes of three TOF planes, each a 'Super-module' consisting of 6 tiles.

### MUON COOLING EXPERIMENTS

High performance muon cooling channels are a critical component for future muon colliders, and to a lesser degree, for future neutrino factories. The first muon cooling experiment, MICE, (Muon Ionization Cooling Experiment) [2] is underway at the Rutherford-Appleton Laboratory (RAL) in the U.K. In addition, a number of design concepts are being considered for cooling channels, and new cooling experiments are needed in the future.

#### MICE Experiment

The layout of the full MICE spectrometers and cooling section is shown in Figure 2. The cooling section consists of 3 hydrogen absorbers and 2 RF sections. The TOFs provide timing information and additional coordinates to improve the measurement by the spectrometers.

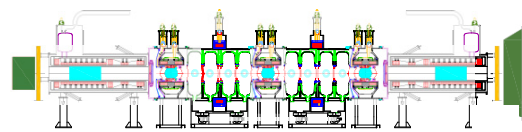


Figure 2: Layout of the full MICE apparatus. Elements 1 and 5 are TOF counters, 2 and 4 are solenoidal spectrometers, and 3 is the cooling channel.

The aim of the MICE experiment is to demonstrate and measure the cooling performance of the cooling channel. The muon beam momentum is 140 to 250 MeV/c.

#### Test of Helical Cooling Channel Performance

Another cooling channel test, MANX, has been proposed as an extension of the MICE experiment. It is

**Advanced Concepts and Future Directions**  
**Accel/Storage Rings 14: Advanced Concepts**

\* Supported in part by SBIR Grant DE-SC00005445

<sup>#</sup>boba247@muonsinc.com

shown in Figure 3, in which thin TOF detectors (TF2 and TF4) may be placed between the solenoidal spectrometers and the matching magnets.

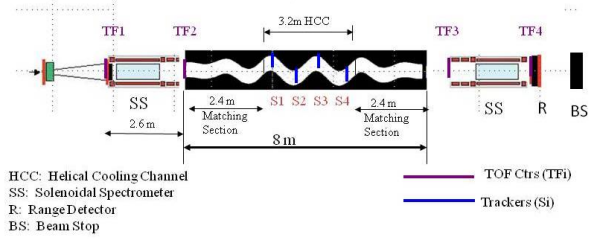


Figure 3: Layout of proposed MANX experiment. A 3.2m long cooling channel and 2 matching magnets are shown between the MICE solenoidal spectrometers. LAPPD TOF detectors, TF1-TF4 are shown.

## STUDY OF RESOLUTIONS WITH TOF AND MAGNETIC SPECTROMETER

### Simulation Configuration

The MICE experiment is proceeding in steps. In the Step II configuration, shown in Figure 4 there is one solenoidal spectrometer with TOF counters upstream and downstream of the solenoidal spectrometer.

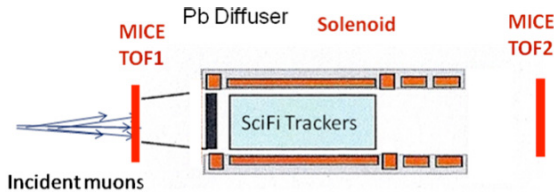


Figure 4: MICE Step II configuration. The SciFi trackers inside the solenoid consist of 5 scintillating fiber planes. The Pb diffuser, whose thickness may vary, produces initial emittances.

The SciFi trackers have spatial resolutions of  $\sim 0.5\text{mm}$  and the TOF detectors consist of two layers of crossed hodoscopes, each slab is plastic scintillator, width 60mm wide and 25 mm thick per layer. The nominal space resolution of the TOFs is  $\sim 17\text{mm}$ , and the time resolution is  $\sim 60\text{ps}$ .

We have simulated the Step II configuration using the g4beamline simulation program [3] to investigate the resolutions for the Step II configuration with the existing TOF counters, and to investigate the dependence of the resolutions on assumed variations of the time and space resolutions for TOF1 and TOF2. In addition we simulated cases in which the LAPPD TOF detectors are placed at the positions of TOF1 and TOF2, and we simulated the case in which no time-of-flight information was used in the fits – SciFi Tracker alone. Preliminary results are presented.

### Simulation Study Method

The simulation results are from a sample of 80,000 muons per case generated, over the momentum range 150 MeV/c to 300 MeV/c. We used the g4beamline track fitting function to use the positions and times of the hits in

the TOF counters and the positions of the hits in the SciFi trackers. The track fitting is done in two passes. In the first pass the trajectory is traced through the system from the generation of the muon to the point the muon exits the system. The path through the magnetic field is calculated using a field map to represent the magnetic field, and the positions, times and momenta are calculated at each detector plane. Energy loss and scattering in the matter is computed. These values are recorded as the “True” values and are saved for the second pass. In the second pass the True values are read in and the assumed time and space resolution parameters of the detectors are used to “smear” the positions and times of the hits in the detectors. Then an iterative fitting routine varies the values and minimizes the overall chi-squared value to achieve a fit. The output of the fit is the final set of values for the positions, times, momenta, and other fit results. These are the “Fit” values. It is then possible to compare the True momenta with the Fit momenta, thus determining the momentum resolution of the system.

### Simulation Results

The first case studied is the use of the SciFi Tracker without supplementary information from the TOF counters. Figure 5(a) shows a plot of transverse momentum resolution RMS ( $\Delta P_T$ ) vs.  $P_T^{\text{True}}$ , where

$$\Delta P_T = P_T^{\text{Fit}} - P_T^{\text{True}}$$

Solenoidal Spectrometer magnetic field to determine the momenta. Figure 5(b) is the corresponding plot for longitudinal momentum resolution RMS ( $\Delta P_Z$ ) vs.

$P_Z^{\text{True}}$ . The spatial resolution used in the fit for the tracker planes was 0.6mm per plane. No time information was used in the fits.

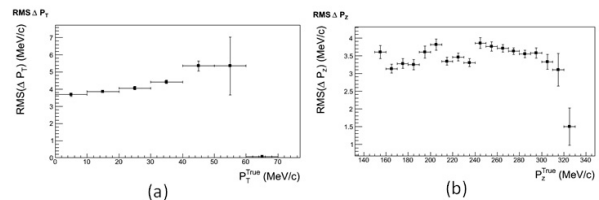


Figure 5: (a)  $P_T$  resolutions vs.  $P_T^{\text{True}}$ , and (b)  $P_Z$  resolutions vs.  $P_Z^{\text{True}}$ , using the SciFi Tracker as a model detector.

One would expect that for constant momentum the  $P_T$  resolution would improve with increasing  $P_Z$ , due to larger radii in the solenoidal field, and wider separation of hits along the transverse circular path. Similarly one would expect that the  $P_Z$  resolution would worsen as a function of  $P_Z$  for constant momentum because the transverse components would decrease as the longitudinal component increases and the radii decrease. We do not

observe this behaviour. Since we have used a broad range of muon momenta from 150 MeV/c to 300 MeV/c, there is a mixture of  $P_T$  values in each  $P_Z$  bin and a mixture of  $P_Z$  values in each  $P_T$  bin, which washes out the effect.

In the second case we show the resolutions for three sets of conditions, using the SciFi Tracker and:

1. TOF counters equivalent to MICE TOF1 and TOF2 in the Step II locations, assuming 60 ps time resolution and 17mm space resolution. The MICE TOFs have ~50mm of plastic scintillator.
2. TOF counters equivalent to MICE TOF1 and TOF2 in the Step II locations, assuming 10 ps time resolution and 0.3mm space resolution.
3. TOF counters equivalent to LAPPD TOF counters at the TOF1 and TOF2 positions in the Step II locations, assuming 10 ps time resolution and 0.3mm space resolution. The LAPPD TOFs have ~6-8 mm of glass equivalent.

Figure 6(a) shows plots of transverse momentum resolution vs.  $P_T^{\text{True}}$  for the three cases and Figure 6(b) shows plots of longitudinal momentum resolution vs.  $P_Z^{\text{True}}$  for the three cases. We see that the curves in Figure 6a are similar in shape to each other, with slightly better  $P_T$  resolution for case of the “fine resolution” MICE TOFs (case 2) compared to case 1, and with case 3 resolutions yielding somewhat bigger improvements over case 2. We do not expect much improvement by adding timing information to the SciFi Trackers to measure transverse momentum.

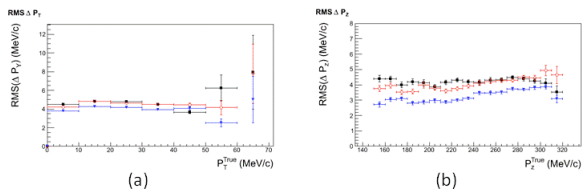


Figure 6: (a)  $P_T$  resolutions vs.  $P_T^{\text{True}}$ , and (b)  $P_Z$  resolutions vs.  $P_Z^{\text{True}}$  for the three conditions: Black points are for case #1, red points are for case #2, and blue points are for case #3.

In Figure 6(b) there is not much difference between case 1 and case 2, and there is a more noticeable improvement in longitudinal momentum resolution vs  $P_Z$

\* These values of resolutions are not characteristic of the MICE TOFs. We are assuming these values only for comparison purposes.

for case 3 over that of case 2. This suggests that the amount of material in the MICE TOFs may be a more important than the assumed time resolution. In case 3 the amount of material is less than in case 2, and the resolutions are assumed to be the same.

Figure 7 shows the  $P_Z$  resolution vs.  $P_T$  and the  $P_T$  resolution vs.  $P_Z$  for the three cases. As in Figure 6 there is less difference between cases 1 and 2 than for case 3.

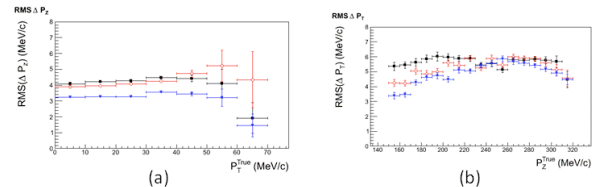


Figure 7: (a)  $P_Z$  resolution vs.  $P_T$ , and (b)  $P_T$  resolution vs.  $P_Z$  for case #1 (black), case #2 (red), and case #3 (blue).

The plots in Figure 7 show about a 20% improvement in the  $P_Z$  resolution for the case of the thinner LAPPD detectors over the thicker MICE TOFs, even when the resolutions are assumed to be identical.

## SUMMARY

We have presented a view of next-generation time-of-flight counters and a preliminary analysis of simulations for a muon cooling experimental configuration. Improvements in the observed resolutions are small as the resolutions are improved and the amount of material in the TOF detectors appears to be a significant contributor to the resolutions. Our simulations were based on a broad spectrum of incident muons, and that has diluted the dependences on the parameters. In addition, although the sample of muons generated was 80,000 in each case, after fitting the number of useful events was lower by a factor of ~10, and the subsequent binning reduced the number of events per bin to a level that made for larger variations in the computations of RMS values. Further analysis with increased statistics is needed.

## REFERENCES

- [1] Large-Area Picosecond Photo-Detectors Project, <http://www.psec.uchicago.edu/>
- [2] MICE web site: <http://www.mice.iit.edu>
- [3] <http://g4beamline.muonsinc.com>